POLITECNICO DI TORINO
Repository ISTITUZIONALE

Application of the Instantaneous Rényi Entropy for Real-Time Damage Detection

(Article begins on next page)

19 April 2024

Application of the Instantaneous Rényi Entropy for Real-time Damage Detection.

Marco Civera[1,*], Erica Lenticchia[1], Gaetano Miraglia[1], Rosario Ceravolo[1], and Cecilia Surace[1]

[1] Department of Structural, Geotechnical and Building Engineering—DISEG, Politecnico di Torino, Corso Duca degli Abruzzi 24, 10129 Turin, Italy
* Correspondence: marco.civera@polito.it

Abstract. Recently, Instantaneous Spectral Entropy (ISE) measurements have been proposed for real-time damage assessment purposes in nonstationary mechanical systems. These include Condition Monitoring (CM) in rotating machinery as well as Structural Health Monitoring (SHM) for civil structures. However, several distinct entropy definitions are available in the scientific literature, each with its advantages and limitations. In the present paper, the potential of the family of Rényi entropies is evaluated. The order α is varied between 0 (corresponding to the Hartley entropy, i.e., the Max-entropy) and $+\infty$ (Min-entropy), encompassing $\alpha \to 1$ (Shannon-entropy) and $\alpha = 2$ (Collision entropy) as particular cases of special interest. The Wigner-Ville (WV), Smoothed Pseudo Wigner Ville (SPWV), Discrete Choi-Williams (DCW), and Continuous Wavelet (CWT) transforms are all tested for the time-frequency (TF) distribution of the target signal. In turn, this TF is used to compute the probability density function, from which the ISE is estimated. A sensitivity analysis is run on all the parameters for each candidate TF transform, aiming at defining the best settings. All studies were performed on a well-known experimental dataset, the three-storey aluminium frame structure developed at the Los Alamos National Laboratories, considering the undamaged conditions as the normality model. The results show good potential for entropy-based real-time damage detection, especially for breathing cracks.

1   Introduction.

Both Structural Health Monitoring (SHM) and Condition Monitoring (CM) can be performed for damage or fault detection with data-driven approaches. In this sense, the current damage diagnosis framework is based on Machine Learning (ML, [1]) principles, especially statistical pattern recognition and outlier detection [2]. The rationale is therefore to link any anomaly in the vibrational behaviour of a target system to occurring damage.

In this context, the Instantaneous Spectral Entropy (ISE) has been recently suggested as a time-varying DSF, with applications for both SHM [3] and CM [4] in real-time [5].

In this study, the family of Rényi entropies [6] is specifically evaluated. These are considered as a generalisation of several well-known entropy definitions, such as the already-cited SSE, the Collision entropy, and the Min- and Max-entropies, depending on the particular value assumed for the order α. Four different TF distributions have been used for the extraction of the instantaneous Rènyi entropies: the Wigner-Ville (WV), Smoothed Pseudo Wigner Ville (SPWV), Discrete Choi-Williams (DCW), and Continuous Wavelet (CWT) transforms. To better address which TF-ISE combination would return the best results (i.e., the highest damage detection capabilities), all these candidates were tested on an experimental dataset. The parameters and settings of each TF candidate were varied as well to test their effects on the final results.

The remaining of this paper is organised as follows: Section 2 briefly recalls the main aspects from the theory of Rényi entropies and the TF transforms applied here. Section 3 describes the experimental case study and Section 4 reports the results. Section 5 summarizes and discusses these results, while the Conclusions end this paper.

2 Theoretical background.

2.1 The Rényi family of entropies.

Firstly introduced by Alfred Rényi in 1961 [6], the Rényi family of entropies can be defined in a single equation, as a function of its order α:

$$H_\alpha = \frac{1}{1-\alpha} \log\left(\sum_{i=1}^{n} p_i^\alpha\right) \tag{1}$$

where n indicates the number of bins (in this context, frequency samples) and p_i is the probability distribution associated with the i-th sample. The generalised formulation of Eq. 1 is valid under the condition that $\alpha \geq 0, \alpha \neq 1$. Regardless of the specific order considered, any member of this family can be used as a quantitative index for the diversity of a system (as is always the case for any entropy measure). Therefore, any values of $\alpha \in [0, +\infty)$ can be considered as a potential candidate for damage diagnosis purposes, accordingly to the eighth axiom of SHM. In this regard, the various Rényi entropies are all maximised for a uniform distribution. On the other hand, they differ in their estimates of the unpredictability for nonuniform distribution. Therefore, they can be compared on a benchmark dataset, to evaluate the appropriateness of each option. Some of these alternatives are well-known and will be discussed in the next subsection.

Some particular cases. The Rényi generalised formulation reported in Eq 1 can assume specific definitions for particular cases of α. These include

$$H_0 = \log n \tag{2}$$

for $\alpha = 0$,

$$H_1 = \lim_{\alpha \to 1} H_\alpha = -\sum_{i=1}^{n} p_i \log p_i \tag{3}$$

for $\alpha \to 1$,

$$H_2 = -\log \sum_{i=1}^{n} p_i^2 \tag{4}$$

for $\alpha = 2$, and finally

$$H_{+\infty} \doteq \min_i (-\log p_i) = -\max_i \log p_i \tag{5}$$

for $\alpha \to +\infty$.

Eq.2 is better known as the Hartley or Max-entropy, firstly introduced in 1928 [7]; Eq. 3 is the already-mentioned SSE, as defined by Powell & Percival in 1979 [8], based on the measure of uncertainty proposed in1948 by Shannon in its seminal work [9]. This is, arguably, the most commonly applied measure of information. Eq. 4 is known as the Collision entropy, or the Rényi entropy par excellence, and can be intended as the probability of two discrete i.i.d. variables to collide, i.e. to casually yield the same value. Finally, Eq. 5 is known as the Min-entropy, since it represents the limit case of the smallest entropy measure in the Rényi family, as it will be discussed in more details later.

Please note that for all formulations, the base 10 logarithm was considered here. This does not affect directly the results; any other base can be used interchangeably. Moreover, all formulations can be further normalised (by dividing them to their respective maximum) to have them confined in the $0 \div 1$ range. For the intent of this research, the -normalised Rényi definition was followed, dividing the results by the logarithm of the number of bins.

For the instantaneous estimation of entropy, p_i must be considered as a function of both frequency and time. This applies to all the definitions (except for Eq. 1, the Max-entropy, which depends only on the number of bins). Therefore, as hinted previously, a time-frequency transform is needed to extract the ISE. This was shown in [3] to greatly affect the results; therefore, several candidates were considered to this aim. The four candidates TF transforms are, specifically, the Wigner-Ville (WV [10]), the Smoothed Pseudo Wigner Ville (SPWV [11]), the Discrete Choi-Williams (DCW [12]), and the Continuous Wavelet (CWT [13]). For the CWT, the Generalised Morse Wavelet (GMW) was utilised as the default mother wavelet. Due to space limitations, these are not described here; the interested reader can refer to the original publications.

3   The experimental benchmark.

The well-known experimental dataset comes from a three-storey structure (Figure 1), built at the Engineering Institute (EI) of the Los Alamos National Laboratory (LANL). This is intended to mimic a scaled shear-type frame structure, typical of high rise buildings. All the technical details regarding the test structure and the experimental setup can be found in [14].

The response of the structures was recorded at four acquisition channels, one per floor (including the base) and located as indicated in Figure 1. All channels were tested for this research; for brevity, only the results of channel #3 will be reported hereinafter. This was found here and in previous studies [3] to be the one most sensitive to structural changes and damage occurrence (at least concerning the entropy of its frequency spectrum).

The original dataset includes one unaltered and sixteen altered cases. These include both simulations of damage as a linear reduction of the stiffness of one or more columns (according to the fully open crack model) or as a pointwise source of bilinearity (following the breathing crack model [15]). This latter case is mimicked by a bumper-column mechanism, which acts as a one-sided constrain, increasing the stiffness along the negative x-direction. This dataset has been widely used in previous researches in the field of SHM [16–18], also including some entropic measurements by Donajkowski et al. [19].

To simulate the time-varying structural changes needed to assess the algorithms for real-time monitoring, the acceleration time series from a subset of the 17 states were considered and concatenated (Figure 2), as suggested in [14]. These states correspond to the #1, #3, #7, #14, #17 states of the original benchmark [14]; their characteristics as enlisted in Table 1. The added masses of states #3 and #17 emulate structural changes unrelated to damage, e.g. transitional operating conditions.

To perform quasi-real-time monitoring, the concatenated signals were framed into 6.4 s-long (2048 timesteps) blocks. The concept, detailed in [3], is to analyse each data packet while the next one is recorded (as the algorithm is proved to run in less than 2 s [3]). This provides an uninterrupted stream of data. As it will be shown in the results, however, this framing affected negatively the instantaneous entropy estimates, due to the edge effects caused by the TF transforms.

The 'Normality Model' of the structural dynamic behaviour, intended to capture the main statistical parameters of the vibrational response under Normal Operating Conditions (NOCs), was defined as follows. Considering Case #1 of the structure as its unaltered state, the ISE extracted from the respective vibration recorded time histories was utilised to define a time-invariant confidence interval. The upper and lower threshold values were set as $\mu_b \pm 2\sigma_b$, where μ_b is the mean of the unaltered baseline and σ_b its standard deviation. That is to say, any datapoint outside of this range has a 95.45% probability of not belonging to the pristine structure.
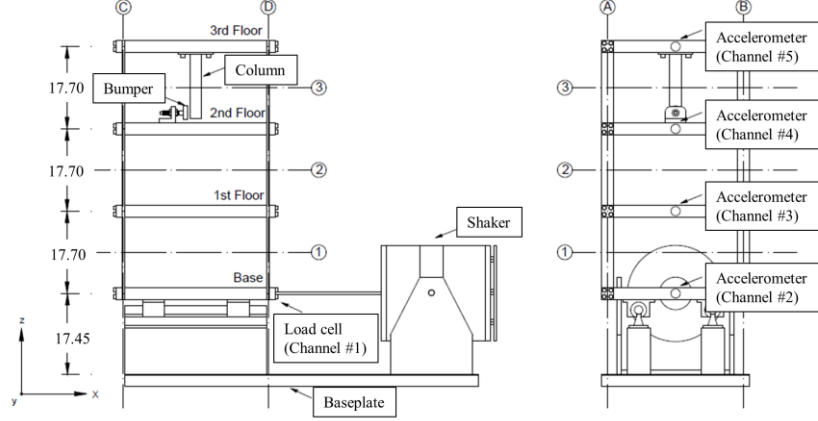
Fig. 1. The LANL three-storey structure. The bumper-column mechanism is visible between the 2nd and the 3rd floor. Adapted from [14]. All measures are reported in cm.

Table 1. Altered and unaltered scenarios for the experimental structure. The cases used for this research are highlighted in bold.

Tract	Original ID [14]	Description
I	#1	Linear baseline.
II	#3	Linear, added mass of 1.2 kg at the first floor.
III	#7	Linear, 87.5% stiffness reduction in two columns of the second interstorey.
IV	#14	Nonlinear, distance between bumper and column tip 0.05 mm.
V	#17	Nonlinear, bumper 0.10 mm from column tip, 1.2 kg added on the first floor.
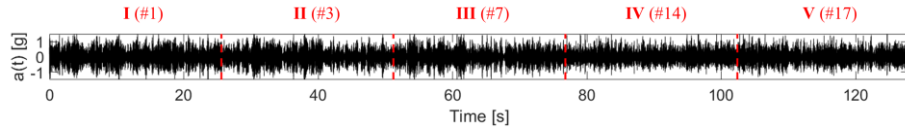
Fig. 2. The concatenated signals, for all the four output channels. The 25th realisation of the unaltered case #1 is shown. The dashed red lines demarcate the five states (1st, 3rd, 7th, 14th, and 17th, in this order).

4 Results.

Seven values of α have been considered: 0.1, $\lim_{\alpha \to 1}$ (i.e. SSE), 2 (i.e. the Collision entropy), 3, 5, 10, and 100. In particular, 100 was considered as indicative of any larger value (up to $+\infty$) since further tests proved that no substantial difference occurred by increasing $\alpha > 100$; thus, it can be considered equivalent to the Min-

entropy. The Max-entropy was discarded a priori, being it – by definition (Eq(2)) – a constant value only related to the number of bins. However, 0.1 was nevertheless tested as a very small order, approaching zero.

The specific results for each TF candidate are reported here below. In all plots, the solid vertical lines indicate the end of the concatenated signals (states #1, #3, #7, #14, and #17) and the dashed lines the end of the single frames (four for each state). The grey area represents the 95.45% confidence interval. The green lines represent the ISE. Due to the high volatility of this index, a moving average was used, computed over $k = 1000$ timesteps. This is indicated by the thick black curves.

4.1 SPWV and WV.

While supposedly more robust than standard WV (for the motivations explained in [3]), the SPWV performed comparably to the WV for all Rényi orders. By way of example, Figure 3 reports the results for α tending to +1 (i.e. for the SSE). On the one hand, the SPWV average was more sensitive to the insertion of the nonlinear mechanism (states #14 and #17). On the other hand, it was characterised by a higher variability, which also returned a larger confidence interval.
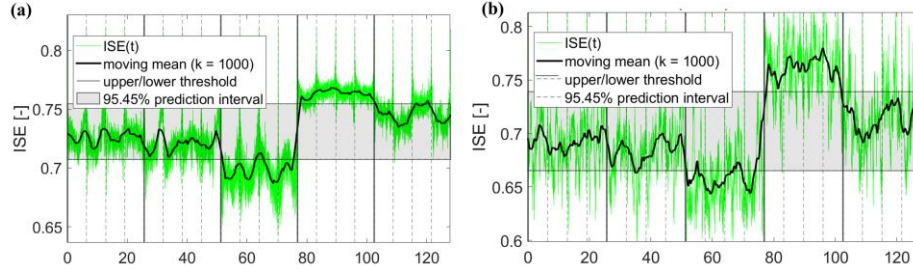

Fig. 3. ISE as extracted from (a) the WV and (b) the SPWV distributions. Rényi entropy of order 1 (SSE), 3rd output channel, 25th realisation.

4.2 DCW.

The sensitivity to the selectivity parameter was tested by varying the value of σ from 0.1 to 1.0 in steps of 0.1. Overall, the sensitivity to damage increased with σ from 0.1 to 0.6 and then inverted its trend, starting to decrease. This seems to suggest that, at least for this application, the value $\sigma = 0.6$, commonly suggested as the default value, is the most viable option, even if by a relatively small margin.

However, in all cases, the DCW was overperformed by both the standard definition of WV and the SPWV. This is visible in the two examples of Figure 4, for $\alpha \to 1$ (SSE) and $\alpha = 2$ (Collision entropy). $\sigma = 0.6$ is reported by way of example; the same aspects described here were encountered for other values of this parameter as well. In fact, in comparison to SPWV and WV, the DCW has slightly better damage detection capabilities; yet these small improvements are overwhelmed by a much higher variability and sensitivity to the detrimental effects of framing. These cause

some false positives in states where the damage (both linear or nonlinear) is not inserted in the system (see e.g. Figure 4.b, second tract, which corresponds to case #3).
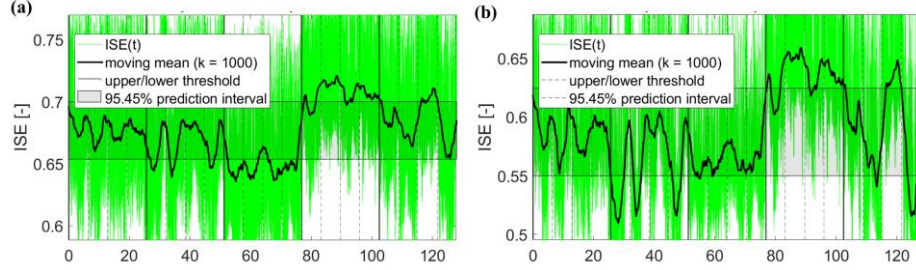
Fig. 4. ISE as extracted from the DCW transform ($\sigma = 0.6$). (a) Rényi entropy of order 1 (SSE), (b) Rényi entropy of order 2 (Collision entropy). 3rd output channel, 25th realisation.

4.3   CWT.

The sensitivity to the two GMW parameters β and γ was tested, following the analyses performed in [4] for an application to rotating machinery. Specifically, β was varied from a minimum value of 2 to a maximum of 40 in steps of 2, while γ was set to 1, 2, 3, or 4, for a total of 140 β/γ combinations.

For all values of α, it was found that increasing γ returned better results, even if the difference for any value $\gamma \geq 3$ is relatively small. This corresponds to a positive skewness of the GMW, for which it becomes more symmetric as β increases.

For constant α and γ, increasing the compactness parameter returned smaller confidence intervals while emphasizing the effects of damage, thus resulting in more effective damage detection. This was particularly evident for $\beta \geq 20$. Therefore, the optimal range of values $\gamma \geq 3, \beta \geq 20$, experimentally defined in [4] for data collected from a wind turbine in operating conditions and using SSE, is confirmed here for this different application and for all the entropies derived from the Rényi generalised definition. Figure 5 reports two examples with $\gamma = 3$ and $\beta = 20$ for $\alpha \to 1$ and $\alpha = 2$ (Figure 5.a and 5.b respectively).

However, it must be remarked that (i) even with optimised parameters, the results obtained by applying the GMW were less effective than the ones obtained with the Bump wavelet in [3] (especially for SSE; for $\alpha = 2$, the optimised GMW is almost on par with the Bump wavelet); (ii) as evidenced in [3], all wavelet-based approaches are largely affected by edge effects and thus by the signal framing. Therefore, they are all less robust than WV and similar approaches.
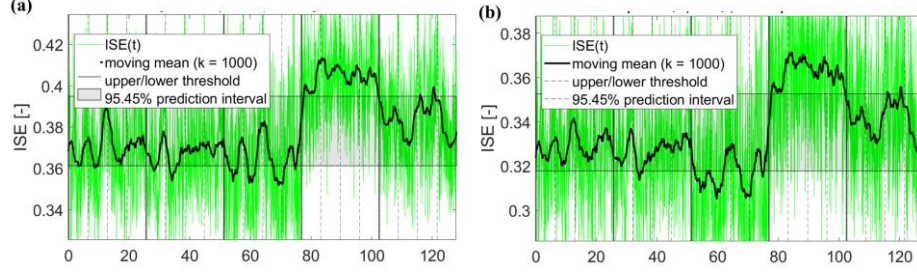
Fig. 5. ISE as extracted from the CWT with GMW as its mother wavelet ($\gamma = 3$ and $\beta = 20$). (a) Rényi entropy of order 1 (SSE), (b) Rényi entropy of order 2 (Collision entropy). 3rd output channel, 25th realisation.

5   Discussion.

As discussed in previous works on the same benchmark dataset [3], the ISE measures proved to be much more sensitive to the added nonlinearity than to the reduced linear stiffness or increased mass. Therefore, the analysis of the results will focus on the capabilities of the different orders of α to capture the occurrence of nonlinear damage.

For all the TF transforms investigated here, it was found that increasing α made the ISE measures more sensitive to the occurrence of damage but also to the detrimental effects of framing. It was already noticed in [3] that the SSE and the Collision entropy performed similarly, which is understandable since they represent very close orders in the Rényi formulations (both were also shown to overperform the Wiener entropy).

For CWT (with GMW parameters set as $\gamma = 3$ and $\beta = 20$), the beneficial additional sensitivity to damage always outweighs the negative additional sensitivity to framing; therefore, the best results were obtained for any value $\alpha \geq 10$, up to $+\infty$.

For WV, a trade-off was reached in between $2 < \alpha < +\infty$, i.e. for orders larger than the Collision entropy but lower than the Min-entropy. After this global optima, the negative framing effects overcome the positive increase in the damage sensitivity.

For DCW (with any σ), the same trend was encountered for the sensibility to the occurrence of nonlinearity. Instead, the sensibility to stiffness reduction decreased monotonically for increasing α. This particular behaviour (reported as well previously in Figure 4) was found only with the DCW.

The same happened at very low orders for the SPWV, where $\alpha \to 1$ (SSE) can be seen as the best option.

These effects of increasing α can be explained by the properties of Eq. 1. One can notice that H_α is non-increasing in α for any given distribution of probability p_i; that is to say,

$$H_0 \geq H_1 \geq H_2 \geq H_{+\infty} \qquad (6)$$

By recalling the definitions provided in Eq 2 – 5, this can be easily proven for all the particular cases of interest here since

$$\log n \leq \sum_{i=1}^{n} p_i \log p_i \leq \log \sum_{i=1}^{n} p_i^2 \leq \max_i \log p_i \qquad (7)$$

The main consequence is that, when α approaches $+\infty$, the Rényi generalised definition becomes increasingly determined by the events with the highest probability. This makes $H_{+\infty}$ the most conservative approach to measure the unpredictability of a set of outcomes for a discrete random variable. This is also clearly understandable from its definition in Eq. 5 as the negative logarithm of the probability of the most likely outcome. It is most probably thanks to this property that $H_{+\infty}$ performed better than other options for CWT and that, in general, increasing the order α returned more sensitive measurements (with all the related advantages and disadvantages).

Regarding the parameter settings for the specific TF transforms, summarizing the results of this and other previous works, one can say that:

- For the CWT with GMW as its mother wavelet, the best results (for all orders) were achieved with $\gamma \geq 3$ and $\beta \geq 20$; however, these were all outperformed by all the other candidate distributions.
- For the DCW, the best results (for all orders) were achieved for $\sigma = 0.6$; however, it was outperformed by both SPWV and WV.
- The SPWV performed better than the DCW but not on par with the WV, despite its supposed improvements with respect to the standard definition.
- Thus, the best overall results were achieved with WV with orders slightly larger than 2, specifically around $\alpha = 3 \div 5$.

6   Conclusions.

The research described here thoroughly investigated the effects of selecting one member of the Rényi family for entropy-based damage detection. In particular, this was applied for real-time SHM, considering the normalised Instantaneous Spectral Entropy (ISE) values. The candidates (which included as special cases the Shannon Spectral, Collision, Hartley, and Min- Entropies) were tested considering different TF distributions, all set with optimised parameters. Overall, no clear best candidate emerged; increasing α returned more damage-sensitive but less stable results. The exact optimum point depends on the specific TF distribution utilised to extract the ISE. Ideally, in absence of edge effects (i.e. if performed without framing), increasing α could increase the sensitivity to damage with no (or limited) adverse effects.

The main outcome of this and previous researches is that ISE measurement can be applied to detect nonlinearities in a nonstationary system. However, for uses as a time-varying damage-sensitive feature, any entropy definition is highly affected by the specific TF distribution given as input. Different TF transforms can lead to very different results, hampering or nullifying the procedure capabilities to detect damage. Thus, the definition of the most proper TF transform is the subject of current and future researches. The uncertainty of the ISE estimates will be investigated as well.

References

1. Farrar CR, Worden K (2013) Structural Health Monitoring: A Machine Learning Perspective

2. Farrar CR, Doebling SW, Nix DA (2001) Vibration–based structural damage identification. Philos Trans R Soc London Ser A Math Phys Eng Sci 359:131–149 . https://doi.org/10.1098/rsta.2000.0717

3. Civera M, Surace C (2022) Instantaneous Spectral Entropy: An application for the Online Monitoring of Multi-Storey Frame Structures. Buildings 12: . https://doi.org/10.3390/buildings12030310

4. Civera M, Surace C (2022) An Application of Instantaneous Spectral Entropy for the Condition Monitoring of Wind Turbines. Appl Sci 2022, Vol 12, Page 1059 12:1059 . https://doi.org/10.3390/APP12031059

5. Bhowmik B, Krishnan M, Hazra B, Pakrashi V (2019) Real-time unified single- and multi-channel structural damage detection using recursive singular spectrum analysis. Struct Heal Monit 18:563–589 . https://doi.org/10.1177/1475921718760483

6. Rényi A (1961) On measure of entropy and information. Proc Fourth Berkeley Symp Math Stat Probab Vol 1 Contrib to Theory Stat 1:547–561

7. Hartley RVL (1928) Transmission of Information. Bell Syst Tech J 7:535–563 . https://doi.org/10.1002/J.1538-7305.1928.TB01236.X

8. Powell GE, Percival IC (1979) A spectral entropy method for distinguishing regular and irregular motion of Hamiltonian systems. J Phys A Gen Phys 12:2053–2071 . https://doi.org/10.1088/0305-4470/12/11/017

9. Shannon CE (1948) A Mathematical Theory of Communication. Bell Syst Tech J 27:379–423 . https://doi.org/10.1002/j.1538-7305.1948.tb01338.x

10. Ville J (1948) Théorie et application de la notion de signal analytique. Cables Transm 2:61–74

11. Yan YS, Poon CCY, Zhang YT (2005) Reduction of motion artifact in pulse oximetry by smoothed pseudo Wigner-Ville distribution. J Neuroeng Rehabil 2:1–9 . https://doi.org/10.1186/1743-0003-2-3/FIGURES/5

12. Choi HI, Williams WJ (1989) Improved Time-Frequency Representation of Multicomponent Signals Using Exponential Kernels. IEEE Trans Acoust 37:862–871 . https://doi.org/10.1109/ASSP.1989.28057

13. Daubechies I, Ingrid (1992) Ten lectures on wavelets. Society for Industrial and Applied Mathematics

14. Figueiredo E, Park G, Figueiras J (2009) Structural Health Monitoring Algorithm Comparisons Using Standard Data Sets. Los Alamos National Lab. (LANL)

15. Bovsunovsky A, Surace C (2015) Non-linearities in the vibrations of elastic structures with a closing crack: A state of the art review. Mech Syst Signal Process 62–63:129–148 . https://doi.org/10.1016/j.ymssp.2015.01.021

16. Civera M, Ferraris M, Ceravolo R, Surace C, Betti R (2019) The Teager-Kaiser Energy Cepstral Coefficients as an Effective Structural Health Monitoring Tool. Appl Sci 9:5064 . https://doi.org/10.3390/app9235064

17. Civera M, Surace C (2021) A Comparative Analysis of Signal Decomposition Techniques for Structural Health Monitoring on an Experimental Benchmark. Sensors 21:1825 . https://doi.org/10.3390/s21051825

18. Martucci D, Civera M, Surace C (2021) The Extreme Function Theory for Damage Detection: An Application to Civil and Aerospace Structures. Appl Sci 11:1716 . https://doi.org/10.3390/app11041716

19. Donajkowski H, Leyasi S, Mellos G, Farrar CR, Scheinker A, Pei J-S, Lieven NAJ (2020) Comparison of Complexity Measures for Structural Health Monitoring. Springer, Cham, pp 27–39